Characterization of Traveling-Wave Josephson Parametric Amplifiers at T = 0.3 K

20 March 2025

This article has been accepted for publication in IEEE Transactions on Applied Superconductivity. This is the author's version which has not been fully edited and content may change prior to final publication. Citation information: DOI 10.1109/TASC.2022.3214656

Characterization of Traveling-Wave Josephson Parametric Amplifiers at T = 0.3 K

V. Granata, G. Avallone, C. Barone, M. Borghesi, S. Capelli, G. Carapella, A.P. Caricato, I. Carusotto, A. Cian, D. Di Gioacchino, E. Enrico, P. Falferi, L. Fasolo, M. Faverzani, E. Ferri, G. Filatrella, C. Gatti, A. Giachero, D. Giubertoni, A. Greco, C. Guarcello, D. Labranca, A. Leo, C. Ligi, G. Maccarrone, F. Mantegazzini, B. Margesin, G. Maruccio, C. Mauro, R. Mezzena, A.G. Monteduro, A. Nucciotti, L. Oberto, L. Origo, S. Pagano, V. Pierro, L. Piersanti, M. Rajteri, A. Rettaroli, S. Rizzato, A. Vinante, and M. Zannoni

***Abstract*— The growing interest in quantum technologies, from fundamental physics experiments to quantum computing, demands for extremely performing electronics only adding the minimum amount of noise admitted by quantum mechanics to the input signal (i.e. quantum-limited electronics). Superconducting microwave amplifiers, due to their dissipationless nature, exhibit outstanding performances in terms of noise (quantum limited), and gain. However, bandwidth and saturation power still show space for substantial improvement. Within the DARTWARS* collaboration, we are developing state-of-the-art microwave superconducting amplifiers based on Josephson junction arrays and on distributed kinetic inductance transmission lines. Here we report the realization of a setup for the characterization of the performances of Josephson Traveling-Wave Parametric Amplifiers (JTWPA) at a temperature of 300 mK. Although in the final experimental setup these amplifiers will operate at a base temperature of about 20 mK, their characterization at 300 mK allows to evidence the main aspects of their performances, but the ultimate noise level. This represents a quick and relatively inexpensive way to test these superconductive devices that can be of help to improve their design and fabrication.**

* **DARTWARS (Detector Array Readout with Traveling Wave AmplifieRS), funded by Italian National Nuclear Institute (INFN), is a quantum technologies project targeted at the development of wideband superconducting amplifiers with noise at the quantum limit and the implementation of a quantum-limited readout in different types of superconducting detectors and qubit.**

***Index Terms*— Superconducting microwave devices, Superconducting device noise, Qubit readout, Quantum computing.**

I. Introduction

Ultra-low noise microwave amplification plays a central role in many fundamental and applied fields, such as experiments for the detection of dark matter, axions [1,2], neutrinos, cosmic radiation, etc., and in quantum computing [3]. These applications require non-dissipative, quantum-limited, and wide bandwidth amplifiers, that can only be realized by employing superconductive devices. The large bandwidth is critical, for in-

Manuscript receipt and acceptance dates will be inserted here. This work was supported by Italian Institute of Nuclear Physics (INFN) through the DARTWARS and QUB-IT projects, by the Institute for Basic Science (IBS-R017-D1) of the Republic of Korea, by the European Union's H2020-MSCA Grant No.101027746, H2020 FETOPEN project SUPERGALAX Grant No. 863313, and EMPIR project PARAWAVE Grant No. 17FUN10, by University of Salerno - Italy under the projects FRB19PAGAN, FRB20BARON, FRB21CAVAL and FRB22PAGAN. *(Corresponding author: Costantino Mauro.)*

V. Granata, G. Carapella, and C. Guarcello are with Physics Dept., University of Salerno, Fisciano (SA), Italy and with INFN - Gruppo Collegato Salerno, Fisciano (SA) 84084, Italy (e-mail: vgranata@unisa.it; gcarapella@unisa.it; cguarcello@unisa.it).

G. Avallone and C. Mauro are with INFN - Gruppo Collegato Salerno, 84084 Fisciano (SA), Italy (e-mail: guavallone@unisa.it; cmauro@na.infn.it).

C. Barone and S. Pagano are with Physics Dept., University of Salerno, Fisciano (SA), Italy, with INFN - Gruppo Collegato Salerno, Fisciano (SA) 84084, Italy and with CNR-SPIN Salerno section, 84084 Fisciano (SA), Italy (e-mail: cbarone@unisa.it; spagano@unisa.it).

M. Borghesi, S. Capelli, M. Faverzani, E. Ferri, A. Giachero, D. Labranca, A. Nucciotti, L. Origo, and M. Zannoni are with Physics Dept., University of Milano-Bicocca, 20126 Milano, Italy and INFN - Sezione di Milano Bicocca, 20126 Milano, Italy (e-mail: matteo.borghesi@unimib.it; silvia.capelli@unimib.it; marco.faverzani@unimib.it; elena.ferri@unimib.it; andrea.giachero@unimib.it; danilo.labranca@mib.infn.it; angelo.nucciotti@unimib.it; luca.origo@mib.infn.it; mario.zannoni@mib.infn.it).

A.P. Caricato, A. Leo, G. Maruccio, A. Monteduro, and S. Rizzato are with Mathematics and Physics Dept., University of Salento, 73100 Lecce, Italy and with INFN – Sezione di Lecce, 73100 Lecce, Italy (e-mail: annapaola.caricato@unisalento.it; angelo.leo@unisalento.it; giuseppe.maruccio@unisalento.it; annagrazia.monteduro@unisalento.it; silvia.rizzato@unisalento.it).

I. Carusotto is with CNR INO, 38123 Povo (TN), Italy and with Physics Dept., University of Trento, 38123, Povo (TN), Italy (e-mail: iacopo.carusotto@ino.cnr.it).

A. Cian, D. Giubertoni, F. Mantegazzini, and B. Margesin are with Fondazione Bruno Kessler, 38123 Povo (TN), Italy and with INFN - TIFPA, 38123 Povo (TN), Italy (e-mail: acian@fbk.eu; giuberto@fbk.eu; fmantegazzini@fbk.eu; margesin@fbk.eu).

D. Di Gioacchino, C. Gatti, C. Ligi, G. Maccarrone, and L. Piersanti are with INFN - Laboratori Nazionali di Frascati, 00044 Frascati (RM), Italy (e-mail: daniele.digioacchino@lnf.infn.it; claudio.gatti@lnf.infn.it; carlo.ligi@lnf.infn.it; giovanni.maccarrone@lnf.infn.it; luca.piersanti@lnf.infn.it).

E. Enrico and L. Oberto are with INRiM - Istituto Nazionale di Ricerca Metrologica, 10135 Torino, Italy and with INFN - TIFPA, 38123 Povo (TN), Italy (e-mail: e.enrico@inrim.it; l.oberto@inrim.it).

P. Falferi and A. Vinante are with Fondazione Bruno Kessler, 38123 Povo (TN), Italy, with INFN - TIFPA, 38123 Povo (TN), Italy and with CNR IFN, 38123 Povo (TN), Italy (e-mail: paolo.falferi@unitn.it; andrea.vinante@ifn.cnr.it).

L. Fasolo and A. Greco are with INRiM - Istituto Nazionale di Ricerca Metrologica, 10135 Torino, Italy and with Politecnico di Torino, 10129 Torino, Italy (e-mail: luca_fasolo@polito.it; angelo.greco@polito.it).

G. Filatrella is with Science and Technology Dept., University of Sannio, 82100 Benevento, Italy and with INFN - Gruppo Collegato Salerno, 84084 Fisciano (SA), Italy (e-mail: filatr@unisannio.it).

R. Mezzena is with Physics Dept., University of Trento, 38123, Povo (TN), Italy and with INFN - TIFPA, 38123 Povo (TN), Italy (e-mail: renato.mezzena@unitn.it).

V. Pierro is with Engineering Dept., University of Sannio, 82100 Benevento, Italy and with INFN - Gruppo Collegato Salerno, 84084 Fisciano (SA), Italy (e-mail: pierro@unisannio.it).

M. Rajteri is with INRiM - Istituto Nazionale di Ricerca Metrologica, 10135 Torino, Italy and with INFN - Sezione di Torino, 10125 Torino, Italy (e-mail: m.rajteri@inrim.it).

A. Rettaroli is with INFN - Laboratori Nazionali di Frascati, 00044 Frascati (RM), Italy (e-mail: alessio.rettaroli@lnf.infn.it).

Color versions of one or more of the figures in this paper are available online at http://ieeexplore.ieee.org.

Digital Object Identifier will be inserted here upon acceptance.

stance, when multiple qubits have to be read with a single amplifier, a stringent requirement for the scaling up of quantum processors. In this perspective, the ultimate performances of the amplifier being crucial, it is essential to optimize their design and fabrication process. Therefore, the availability of a quick and simple methodology to characterize these ultra-low noise cryogenic superconductive amplifiers is of paramount importance to speed up their development.

In this work we report the realization of a setup for the characterization of the performances of Josephson Traveling-Wave Parametric Amplifiers (JTWPA) at a temperature of 300 mK. Such operating temperature can be easily reached with a relatively simple ^{3}He-based cryogenic insert, with proper modification to allow the appropriate RF connections.

In the following a basic introduction to the JTWPA principle of operation will be given (Section II). Then the aspect related to the design and fabrication of a specific realization of JTWPA will be discussed (Section III). In Section IV the setup of the test station will be described in detail and in section V some preliminary results on the Josephson junction characterization will be reported.

II. The Josephson Travelling Wave Parametric Amplifier

Modern quantum computers process very fast signals, having bandwidth of several GHz and amplitude in the order of the μV and, consequently, demand low-noise amplifiers with wide bandwidth. Amplifiers with these characteristics are also required in fundamental physics experiments such as axion detection [2].

Semiconductor transistors-based amplifiers are widely employed [4, 5, 6], as they have a good bandwidth in the microwave frequency range, but, their intrinsically dissipative nature limits the achievable noise performances. In terms of noise temperature, their current limit is in the range of 2-5 K [6], while for quantum computing application, it should stay below 1 K [7].

Amplifiers based on superconductive devices, being essentially non-dissipative, represent an unavoidable choice. In this scenario, Josephson Parametric Amplifiers (JPAs) were introduced to meet these needs [3, 8, 9, 10, 11]. They are currently the most used in the field of quantum technologies as they can reach the quantum noise level. A typical JPA consists of a superconducting quantum interference device (SQUID) combined with a superconducting coplanar waveguide resonator. The combined system acts as a tunable non-linear microwave resonator. Non-linear microwave resonator tuning can be exploited to parametrically pump the JPA by applying a strong microwave signal at twice the resonant frequency. However, while achieving good gain and excellent noise performance, JPAs suffer from a limited bandwidth (few hundred megahertz) [7, 12], which can be a problem for multiplexing many qubits conversely requiring a wide bandwidth (several gigahertz) [3]. JPAs are also used in fundamental physics experiments, but also in this case the limited bandwidth of the amplifiers does not allow a simple scaling up of the experiments.

To overcome the limitations of JPA, a device, called **Josephson Traveling Wave Parametric Amplifier**, has been developed, showing improved performances [13, 14, 15]. Basically, it consists of a discrete elements transmission line formed by an array of cells made by Josephson junctions or SQUID [13, 16, 17, 18, 19, 20] (acting as nonlinear inductor) and a capacitive shunt to the ground. Model calculations have shown that JTWPAs can have quantum limited noise, wide bandwidth, and high gain.

Superconducting JTWPAs are based on the parametric amplification of microwaves traveling along the transmission line, where the Josephson junctions, or SQUIDs, represent the nonlinear elements [21]. Like other parametric amplifiers, JTWPAs transfer power from a strong microwave signal (called a pump) to a weaker one (called a signal). The dependence of the Josephson inductance on current is responsible for mixing and parametric amplification.

In parametric amplifiers, a large amplitude pump signal is sent at the frequency f_p, together with the weak signal to be amplified, at the frequency f_s. The pump signal current modulates the non-linear inductance, coupling the pump to the signal, and, if the JTWPA is suitably designed, produces, by mixing in frequency, an amplification of the signal at frequency f_s, as well as the generation of an idler signal at a frequency f_i. It is possible to obtain different mixing processes, depending on the non-linearity of the dependence of the cell inductance L_J on the current I. The first process, called *degenerate four-wave mixing* (4WM), is triggered by a quadratic current dependence of the nonlinear inductance [20]. In such case the relation between the involved frequencies is:

$$2f_p = f_s + f_i \tag{1}$$

The second process, called *three-wave mixing* (3WM), depends on the presence of a linear current dependence of the nonlinear inductance [22], and the relation between the involved frequencies is:

$$f_p = f_s + f_i \tag{2}$$

Depending on the design of the array cells, JTWPA can operate either in 4WM or in 3WM mode. By using a DC magnetic field, or a DC bias current, it is possible to modify the intrinsic nonlinearity and switch from one mode to the other.

The 3WM mode is normally preferable because the pump frequency can be easily filtered out from the output of the amplifier, being far enough from the signal and idler frequencies. This prevents the saturation of subsequent electronic amplification stages due to the large power of the pump signal.

Conversely, in the 4WM mode the pump frequency lies in between the signal and idle frequencies, resulting in a gain "hole" at the center of the amplifier bandwidth.

JTWPAs can achieve gain higher than 20 dB, bandwidth wider than 3 GHz and noise level below 0.7 K making them the natural choice for simultaneous readout of several dozens of qubits [19]. However, as the pump, the signal and the idle tones travel along the transmission line, a phase mismatch is slowly

This article has been accepted for publication in IEEE Transactions on Applied Superconductivity. This is the author's version which has not been fully edited and content may change prior to final publication. Citation information: DOI 10.1109/TASC.2022.3214656

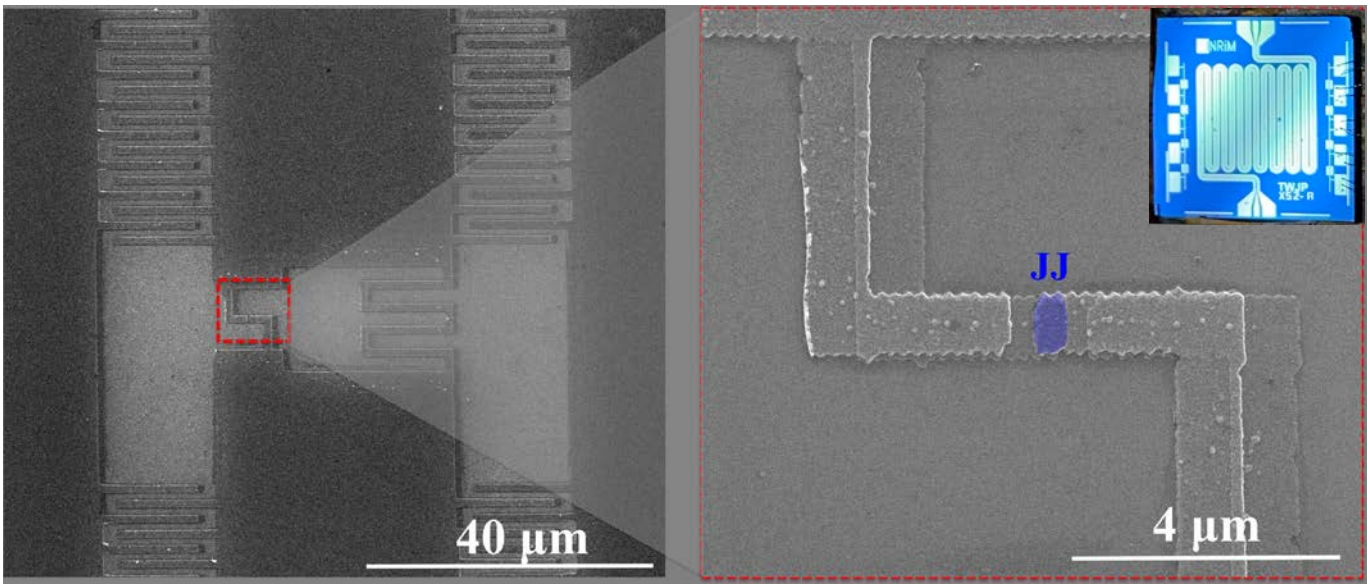

Fig. 1. Field Emission Scanning Electron Microscopy (FESEM) images of one cell of the JTWPA sample (X52_A). To the left: the elementary cell, formed by an RF-SQUID and an inter-digital capacitor to ground. To the right: an enlarged view of the overlapped electrodes forming the Josephson junction (highlighted in blue and indicated as JJ); in the inset a picture of the whole chip with the transmission line made of 990 cells.

accumulated., leading to a limitation of the maximum achievable gain. To avoid this problem, as well as to limit the effects of harmonics of the pump tone, several approaches to achieve a phase matching condition have been proposed [16, 17, 20, 22, 23] which, however, in many cases significantly complicate the overall transmission line design.

III. Sample Fabrication

The JTWPAs realized within the DARTWARS collaboration and analysed in the present manuscript are entirely produced by standard Al deposition utilising a single lithographic step. Details of the design are reported in [21]. For the fabrication of the Josephson junctions (JJs), cores of the JTWPAs, a double angled evaporation is used [24, 25], so as to create an overlap between two superconducting leads, hence the junction area, by the superposition of two distinct metal layers produced by two separated depositions (see right panel of Fig. 1). Once defined the critical current density as I_c divided by the cross-sectional area S of the superconducting region $J_c = I_c / S$, and the critical current I_c as the transport current at which we clearly get the flow voltage, the creation of the oxide layer between the two leads of the junctions is of fundamental importance, since it is directly related to the critical current density and the associated junction capacitance. Its creation takes place through an oxidation process of the first Al layer operated using a continuous flow of pure oxygen, in a vacuum chamber where the pressure is under constant control. There is indeed a direct relation between the oxidation time, the oxidation pressure and the critical current density of a JJ, that allows to predict with a certain precision the critical current of a JJ given the oxidation conditions and the overlap area). The critical current density of a JJ can be considered a function of the $\sqrt{P} \cdot t$ product [26], where P is the oxidation pressure while t is the oxidation time. Indeed the easiest and more accurate way to obtain the J_c vs $\sqrt{P} \cdot t$ relation is to directly measure the critical currents of JJs with known area, and then build an experimental curve that interpolates the measured data (see Fig. 2). Fig. 1 shows a micrograph of a typical Al-based JJ realised by the shadow mask evaporation technique.

The measurements of the critical currents to create the J_c vs $\sqrt{P} \cdot t$ curve were performed in a wet dilution refrigerator model CF-MCK50-100 from Leiden Cryogenics BV with a base temperature of 50 mK. The Current-Voltage (I-V) characteristics were measured through a 4-terminal scheme, where the junction is powered by a voltage source Yokogawa GS200 in series with a resistor with resistance R = 10 kΩ. The current supplied is then measured through a transimpedance amplifier FEMTO DDPCA-300 with gain $Z = 10^5$ V/A, of which the output voltage is measured using a multimeter Keithley 2400. The voltage drop across the junction is measured using a second Keithley 2400, preamplified by a voltage amplifier Aivon dVPA-B with gain G = 100. Both the current and voltage lines are filtered with RC low pass filters with 10 MHz and 30 Hz cutoff frequency, respectively.

The relation between the oxidation pressure, oxidation time and critical current density can be deduced through the $\sqrt{P} \cdot t$ rule studied in [26, 27]. In the microscopic theory of the Josephson effect, the relation between the critical current density and the width of the potential barrier of a JJ is found to be [28]

$$J_c = \frac{e\hbar k}{m_e} \frac{\sqrt{n_1 n_2}}{\sinh(2kd)} \tag{3}$$

Where e is the elementary charge, $\hbar = h/2\pi$ is the reduced Planck constant, d the width of the potential barrier, m_e is the electron mass, $n_{1,2}$ are the supercarrier densities in the two leads

of the JJ and *k* is the decay constant of the barrier. We can obtain the equation for the thickness of the barrier as a function of the $\sqrt{P} \cdot t$ product in terms of the extended Cabrera-Mott theory [26] for the formation of very thin oxide films as

$$d^{3/2} = 6.05\, log\left(138 \cdot P^{1/2} \cdot t + c\right) \quad (4)$$

where *d* is the thickness of the oxide barrier in Å, *c* is a fitting dimensionless constant, while pressure and time are expressed in torr and min, respectively. Combining (4) and (3) leads to

$$J_c = \frac{ak}{sinh\left(2k\left[6.05\, log\left(138 \cdot P^{1/2} \cdot t + c\right)\right]^{2/3}\right)} \quad (5)$$

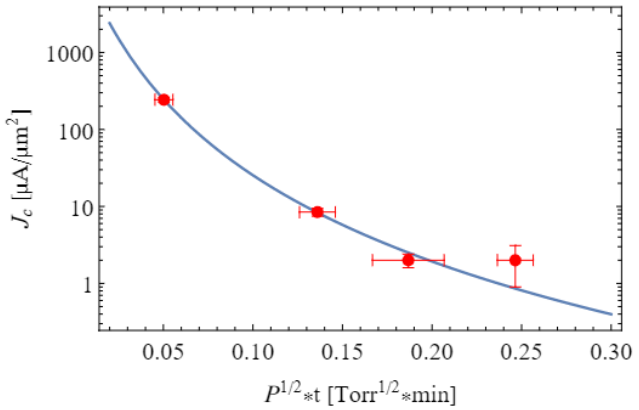

Fig. 2. Dependence of the Josephson critical density on oxidation parameters ($\sqrt{P}$·t). The blue curve represents a polynomial best fit.

where a =1.3 · 10^6 μA · Å is a constant valid for Al-based JJs at T = 0 K.

We performed 4 measurement sessions, in each of which we measured between 10 and 15 Josephson critical currents relative to the same oxidation process, but with different time and pressure values. In Fig. 2 we report an experimental dataset modelled with (5), where each point corresponds to a different measurement session.

The measurements reported in Fig. 2 have uncertainty on the $\sqrt{P}\,t$ axes given mainly by the pressure fluctuations recorded during the oxidation processes, and on the J_c axes calculated as the standard deviation on the whole number of measurements performed during the different runs.

The critical currents considered in the following section are the expected currents for the JJs embedded in the transmission line of the JTWPA labelled JTWPA_X52. Their areas are designed to be A= 0.4 μm^2. Hence, exploiting the calibration curve reported in Fig. 2, with an oxidation process lasting for 10 minutes at 3.50 · 10^{-4} Torr, they should result in a critical current I_c= J$_c$ · A ≈ 6.6 μA/μm^2 · 0.4 μm^2 ≈ 2.6 μA. Furthermore, exploiting Eq. 4 and considering the relative dielectric constant of *Al* (ϵ_r= 9) their capacitance should result in C= $\epsilon_0 \cdot \epsilon_r \cdot A$ / d ≈ 29.3 fF.

IV. Experimental Setup

The experimental setup to test a JTWPA is rather critical and demands for a careful tuning of the temperature, RF signals and DC lines. In the following, the specific experimental setup used is described.

A. RF section setup

A 0.01-20 GHz signal generator (SMP02 from Rohde&Schwarz) is used for the pump signal. The output signal level is attenuated by a 20 dB attenuator. This and further attenuator stages are essential to bring the signal level in the range of operativity of the parametric amplifier (around -60/-80 dBm). The output feeds one input of a 20 dB directional coupler, whilst the other coupler input is driven by a 0.01-19 GHz signal generator based on Texas Instruments LMX2595 RF synthesizer acting as main signal, via a 0-10 dB HP manual step attenuator. The combined pump and signal tones, after a 0-90 dB HP manual step attenuator, enter the cryogenic insert through a 30 dB fixed attenuator. In this way it is possible to set independently the frequency and amplitudes of the pump and signal tones.

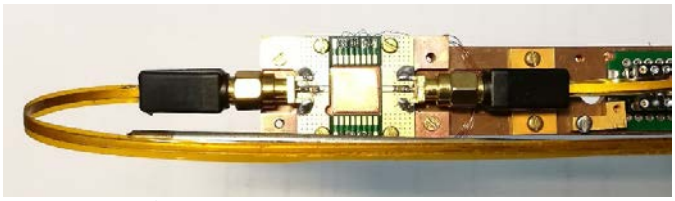

Fig. 3. A detail of the cold part with the custom sample holder, the accommodation pad for the JTWPA chip at the center, and the RF cables attached.

Once in the cryogenic insert, the combined pump and signal tones reach the JTWPA, placed in a custom sample holder shown in Fig. 3, through a series of cables and attenuators. The amplifier output is connected, through low thermal conductivity RF cables, to a 0.3-14 GHz cryogenic low noise amplifier from Low Noise Factory, thermally anchored at the 4 K stage, having a gain of 35 dB. The output of the cryogenic amplifier is connected, through a stainless steel coaxial cable, to the SMA port of the cryogenic insert, where a room temperature low noise amplifier further boosts the signal that is then sent to a spectrum

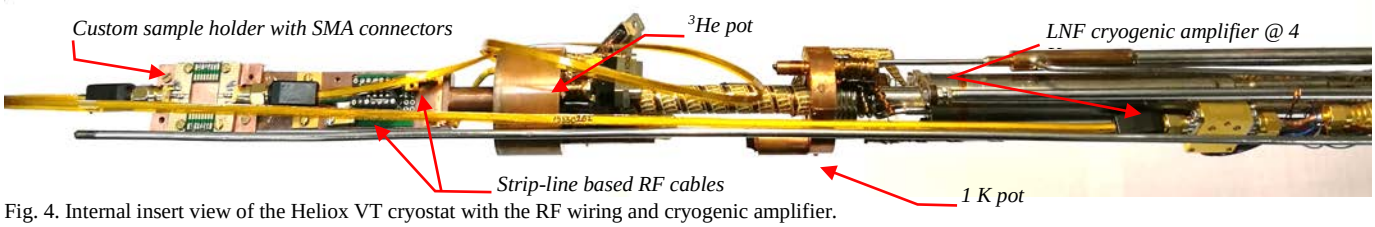

Fig. 4. Internal insert view of the Heliox VT cryostat with the RF wiring and cryogenic amplifier.

This article has been accepted for publication in IEEE Transactions on Applied Superconductivity. This is the author's version which has not been fully edited and content may change prior to final publication. Citation information: DOI 10.1109/TASC.2022.3214656

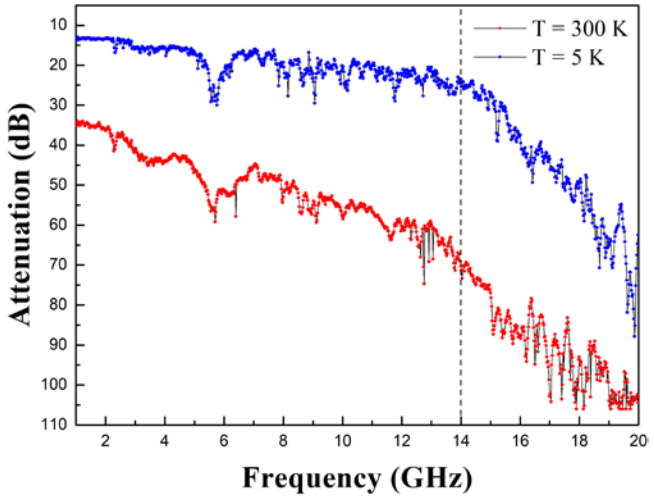

Fig. 5. In-out measurement of RF attenuation without sample (red curve: T = 300 K; blue curve: T = 5 K; dashed line: upper limit of cryogenic amplifier's working frequency).

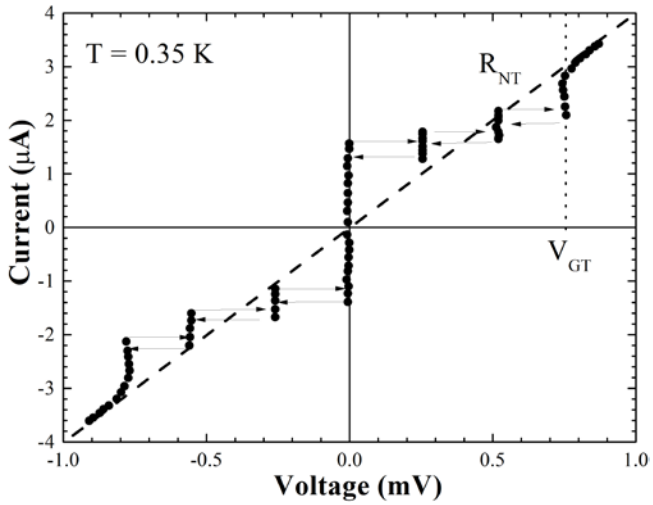

Fig. 6. Current-Voltage curve of a test series array of JJs recorded at T = 0.35 K. The arrows show the switching events during looping of bias current. The dashed line is the total normal resistance. The dotted line is the total gap sum voltage.

analyzer (9 KHz – 26 GHz 8653E from HP) for investigating its spectral properties.

B. DC section setup

The DC section is based on homemade low noise DC bias and low frequency amplifiers designed to DC bias the JTWPA and other test structures present on the chip and record theirs DC current-voltage characteristics. The electronic box is enclosed in a cast aluminium box and connected, through carefully shielded cables, to the cryogenic insert, where low heat conductivity cables run down to the low temperature stage up to the chip to be tested. To avoid possible damage of the JJs in the chip by electrostatic discharge (ESD), removable shorts to ground are provided on each signal line.

C. Base cryogenic setup

The cryogenic section of the experimental setup is built around the ^{3}He insert HelioxVL from OXFORD Instruments.

As declared by the manufacturer, the system is capable of a base temperature of 245 mK for more than 90 hours, with a 40 μW of cooling power available to the sample at 290 mK for more than 10 hours. After this time, the temperature of the system is no more under control, now depending mainly on the mass load and the isolation properties of the dewar. The insert is equipped with two RF lines thermalized down to the 4K stage. The coaxial cables are semi-rigid stainless steel with an attenuation of ~ 15 dB/m in the range 1-11 GHz. A picture of the lower temperature part of the insert is shown in Fig. 4, where also part of the RF setup is shown.

The major limitation of this system is the small sample volume available, that strongly limits the number and type of microwave components that can be integrated.

D. Improved cryogenic setup

In order to be able to properly test the JTWPA, the basic setup of the cryostat have been modified in the RF section. Great attention has been given to thermal issues and to avoid electro-magnetic interferences. A dedicated sample holder, made by high quality oxygen free copper, (see Fig. 3) has been designed and engineered. It must provide optimal thermal coupling while holding a low mass so to be economical on the available cooling power. For the same reason we have opted for the use of special low thermal conductivity Cri/oFlex® 2 RF cables by Delft Circuits to connect the JTWPA to the RF in and out lines. Moreover, these strip-line based cables exhibit a decreasing roll-off while lowering the temperature.

To test the effect of all RF connections at room temperature and at 5 K, the overall in-out attenuation has been measured, bypassing the JTWPA with a short SMA adapter but leaving the cryogenic amplifier (see Fig. 5). Beside an adsorption peak at about 5 GHz, due to standing waves resonances induced by the series of RF connections, the overall behavior at 5 K shows a smooth increase of attenuation limited to about 12 dB in the range of frequency 1 - 14 GHz (the bandwidth of the cryogenic amplifier), resulting in more linear spectra too. Here has to be stressed that the differences between measured attenuations at 5 K and at 0.3 K are expected to be small and not frequency dependent. Moreover, these can be easily compensated by the external attenuators. At room temperature the attenuation is much larger, as expected from the RF cables specs. It is worth noting that, after the early measurements, we observed strong RF couplings between input and output signals resulting in a distorted and ghost signal (i.e. a replica of a particular signal, frequency shifted that is mixed to the input signal). This issue has been solved by wrapping the SMA connectors of the RF cable with adhesive aluminum foil, so to minimize the effects of electromagnetic interferences.

As final remark regarding the RF setup, we note that the path and thermalization of the strip-line based RF cables is critical in terms of heat load. If not carefully chosen, it may create thermal link among different stages, preventing the system from reaching the nominal base temperature (T = 0.3 K).

V. DC Characterization

To test junction quality, simple devices with electrical characteristics previously reported are fabricated on the same chip as the JTWPA sample.

In Fig. 6 we show the I-V curve of one of such test devices, consisting of a series array of three JJs with dimensions nominally identical to the single junctions of elementary cells of the JTWPA shown in Fig. 1. The I-V curve is recorded at 0.35 K and external magnetic field is shielded by a cryoperm foil. Sweeping the bias current from positive to negative values and vice versa, we observe three slightly different critical currents and similar gap voltages. The small back bending envisaged at total gap voltage V_{GT} is commonly observed in the I-V characteristic of small Al/AlO$_x$/Al JJs [29], and it is possibly accounted for a non equilibrium superconductivity [30] phenomenon.

The mean critical current is about I_c = 2 μA, the lower is 1.8 μA, the higher is 2.2 μA. The total gap voltage at this temperature is found to be V_{GT} = 0.75 mV, meaning a mean gap voltage per single junction of V_G = 250 μV.

Assuming the superconducting gap at work temperature $\Delta(T$ = 0.35 K) almost saturated to the $\Delta(0)$ value [31], from relation [30] $eV_G = 2\Delta = 3.52\, K_B T_c$ we estimate a critical temperature of our thin aluminum close to T_c = 0.9 K.

The total normal resistance is found R_{NT} = 250 Ω, from which we estimate a normal state resistance per single junction of about R_N = 83 Ω, giving a characteristic product I_cR_N = 200 μV. For an ideal tunnel junction the characteristic product is related to the gap voltage by relation [30] $I_cR_N^{(th)} = V_G \cdot \pi/4$. From measured mean I_c and V_G we expect $R_N^{(th)}$ = 100 Ω, instead of the measured R_N = 83.3 Ω. Such a discrepancy suggests that a parallel resistive leakage (estimated resistance about R_L = 500 Ω per junction) is present in our junctions.

The presence of leakage in small area and high or moderately high critical current density junctions (in our case J_c = 400 A/cm^2) often results [32] in a strong reduction of hysteresis, as, in fact, can be appreciated also in the I-V of our junctions shown in Fig. 6. Such leakage currents could be possibly accounted for the granularity of the deposited films (see right panel of Fig. 1), resulting in non uniform barrier thickness, and by the shadow mask technique used to fabricate the junctions. The non uniform barrier thickness can also result in localized nanoshorts (pinholes) that apparently increase the measured critical current. We cannot exclude the presence of such pinholes in the test device, as suggested by a measured critical current slightly larger than the nominally expected critical current value I_c = 1.3 μA.

Finally, the shadow mask technique normally produces a reduction of the film thickness at junction edges often resulting in severe reduction of critical temperature in these regions. So, at edges, a SIN or also a NIN junction could form and resistively shunts the bulk SIS junction. Currently, we are trying to reduce both the granularity of the films and the edge wedging effects, responsible of some undesired non idealities.

VI. Conclusion

JTWPAs are promising superconductive devices for ultimate performances as quantum limited amplifiers in the microwave region from 1 to 20 GHz. Although their operation is typically at temperatures well below 100 mK, we have shown that it is possible to optimize a setup to characterize JTWPA at 300mK, where they are already cold enough to show their ultimate performances being the JTWPA typically realized with aluminum, also in consideration that quantum noise temperature level at 10 GHz is about 0.5 K. Together with the details of the sample fabrication, the cryogenic and microwave experimental setup, we have shown some preliminary DC characterization of the JJ used in the JTWPA. The obtained results can provide quick feedback for the optimization of the design and of the fabrication of these type of superconductive amplifiers.

References

[1] C. Bartram *et al*. (ADMX Collaboration), "Axion dark matter experiment: Run 1B analysis details", *Phys. Rev. D*, vol. 103, February 2021, pp. 032002, doi: 10.1103/PhysRevD.103.032002.

[2] D. Alesini et al., "Galactic axions search with a superconducting resonant cavity", *Phys. Rev. D*, vol. 99, May 2019, pp. 101101(R), doi: 10.1103/PhysRevD.99.101101.

[3] P. Krantz *et al*., "A quantum engineer's guide to superconducting qubits," *Appl. Phys. Rev.*, vol. 6, no. 2, May 2019, Art. no. 021318, doi: 10.1063/1.5089550.

[4] W. R. Deal *et al.*, "Low noise amplification at 0.67 THz using 30 nm InP HEMTs," *IEEE Microw. Wirel. Compon. Lett.*, vol. 21, no. 7, pp. 368–370, Jun. 2011, doi: 10.1109/LMWC.2011.2143701.

[5] J. Schleeh *et al*., "Ultralow-power cryogenic InP HEMT with minimum noise temperature of 1 K at 6 GHz," *IEEE Electron Device Lett*., vol. 33, no. 5, pp. 664–666, May 2012, doi: 10.1109/LED.2012.2187422.

[6] J. Schleeh *et al*., "Cryogenic noise performance of InGaAs/InAlAs HEMTs grown on InP and GaAs substrate," *Solid-State Electron*., vol. 91, pp. 74-77, Jan. 2014, doi: 10.1016/j.sse.2013.10.004.

[7] J. Aumentado, "Superconducting parametric amplifiers: The state of the art in Josephson parametric amplifiers," *IEEE Microw. Mag.*, vol. 21, no. 8, pp. 45–59, Aug. 2020, doi: 10.1109/MMM.2020.2993476.

[8] N. Bergeal *et al*., "Analog information processing at the quantum limit with a Josephson ring modulator," *Nature Phys.*, vol. 6, pp. 296–302, Feb. 2010, doi: 10.1038/nphys1516.

[9] T. Yamamoto *et al*., "Flux-driven Josephson parametric amplifier," *Appl. Phys. Lett.*, vol. 93, no. 4, Jul. 2008, Art. no. 042510, doi: 10.1063/1.2964182.

[10] T. Roy *et al*., "Broadband parametric amplification with impedance engineering: Beyond the gain-bandwidth product," *Appl. Physics Lett*., vol. 107, no. 26, Dec. 2015, Art. no. 262601, doi: 10.1063/1.4939148.

[11] J. Y. Mutus *et al.*, "Design and characterization of a lumped element single-ended superconducting microwave parametric amplifier with on- chip flux bias line," *Appl. Phys. Lett.*, vol. 103, no. 12, Sep. 2013, Art. no. 122602, doi: 10.1063/1.4821136.

[12] F. Lecocq *et al*., "Nonreciprocal microwave signal processing with a field-programmable Josephson amplifier," *Phys. Rev. Appl*., vol. 7, no. 2, Feb. 2017, Art. no. 024028, doi: 10.1103/PhysRevApplied.7.024028.

[13] O. Yaakobi *et al.*, "Parametric amplification in Josephson junction embedded transmission lines," *Phys. Rev. B*, vol. 87, no. 14, Apr. 2013, Art. no. 144301, doi: 10.1103/PhysRevB.87.144301.

[14] M. Trepanier *et al*., "Realization and modeling of metamaterials made of rf superconducting quantum-interference devices," *Phys. Rev. X*, vol. 3, no. 4, Oct. 2013, Art. no. 041029, doi: 10.1103/PhysRevX.3.041029.

[15] M. A. Castellanos-Beltran and K. W. Lehnert, "Widely tunable parametric amplifier based on a superconducting quantum interference device array resonator," *Appl. Phys. Lett.*, vol. 91, no. 8, Aug. 2007, Art. no. 083509, doi: 10.1063/1.2773988.

[16] K. O'Brien *et al.*, "Resonant phase matching of Josephson junction traveling wave parametric amplifiers," *Phys. Rev. Lett.*, vol. 113, no. 15, Oct. 2014, Art. no. 157001, doi: 10.1103/PhysRevLett.113.157001.
[17] T. C. White *et al.*, "Traveling wave parametric amplifier with Josephson junctions using minimal resonator phase matching," *Appl. Phys. Lett*., vol. 106, no. 24, Apr. 2015, Art. no. 242601, doi: 10.1063/1.4922348.
[18] M. T. Bell and A. Samolov, "Traveling-wave parametric amplifier based on a chain of coupled asymmetric SQUIDs," *Phys. Rev. Appl.*, vol. 4, no. 2, Aug. 2015, Art. no. 024014, doi: 10.1103/PhysRevApplied.4.024014.
[19] C. Macklin *et al.*, "A near-quantum-limited Josephson traveling-wave parametric amplifier," *Science*, vol. 350, no. 6258, pp. 307–310, Sep. 2015, doi: 10.1126/science.aaa8525.
[20] E. Jeffrey *et al.*, "Fast accurate state measurement with superconducting qubits," *Phys. Rev. Lett.*, vol. 112, no. 19, May 2014, Art. no. 190504, doi: 10.1103/PhysRevLett.112.190504.
[21] S. Pagano *et al.*, "Development of quantum limited superconducting amplifiers for advanced detection," *IEEE Trans. Appl. Supercond.*, vol. 32, no. 4, Jun. 2022, Art. no. 1500405, doi: 10.1109/TASC.2022.3145782.
[22] A. B. Zorin, "Josephson traveling-wave parametric amplifier with three-wave mixing," *Phys. Rev. Appl.*, vol. 6, no. 3, Sep. 2016, Art. no. 034006, doi: 10.1103/PhysRevApplied. 6.034006.
[23] R. W. Klopfenstein, "A transmission line taper of improved design," in *Proceedings of the IRE*, vol. 44, no. 1, pp. 31-35, Jan. 1956, doi: 10.1109/JRPROC.1956.274847.
[24] G. J. Dolan, "Offset masks for lift-off photoprocessing," *Appl. Phys. Lett.*, vol. 31, no. 5, pp. 337–339, 1977, doi: 10.1063/1.89690.
[25] T. A. Fulton and G. J. Dolan, "Observation of single-electron charging effects in small tunnel junctions," *Phys. Rev. Lett.*, vol. 59, no. 1, pp. 109–112, Jul. 1987, doi: 10.1103/PhysRevLett.59.109.
[26] J. E. Boggio, "The pressure dependence of the oxidation of aluminum at 298 °K," *Surface Science*, vol. 14, no. 1, pp. 1–6, Mar. 1969, doi: 10.1016/0039-6028(69)90041-7.
[27] L. Wang. "Fabrication stability of Josephson junctions for superconducting qubits," *Technische Universitat Munchen*, 2015.
[28] A. Barone and G. Paternò, "*Physics and applications of the Josephson effect*," Wiley, New York, 1982.
[29] Lan Dong *et al.*, "Fabrication of Al/AlO_x/Al junctions using pre-exposure technique at 30-keV e-beam voltage", *Chinese Phys. B*, vol. 25, no. 8, Jun. 2016, Art. no. 088501, doi: 10.1088/1674-1056/25/8/088501.
[30] Tinkham, "*Introduction to Superconductivity*," second edition, Dover Publications, 2004.
[31] N. A. Court, A. J. Ferguson, and R. G. Clark, "Energy gap measurement of nanostructured aluminium thin films for single Cooper-pair devices," *Supercond. Sci. Technol.*, vol. 21, no. 1, Jan. 2008, Art. no. 015013, doi: 10.1088/0953-2048/21/01/015013.
[32] R. E. Howard *et al.*, "Small-area high-current-density Josephson junctions," *Appl. Phys. Lett*., vol. 35, no 11, pp. 879–881, Dec. 1979, doi: 10.1063/1.90991.